The International Journal of Advanced Manufacturing Technology (2022) 121:7569–7589
https://doi.org/10.1007/s00170-022-09795-9

ORIGINAL ARTICLE

The effect of temperature field on the characteristics of carbon fiber reinforced thermoplastic composites in the laying and shaping process

Fuhai Zhao[1] · Zhiqiang Liu[1] · Rifan Chen[1] · Yi Hao[1] · Zhihao Ma[1]

Received: 26 April 2022 / Accepted: 14 July 2022 / Published online: 1 August 2022

Abstract
This work investigates the temperature field during the automated layup of carbon fiber reinforced thermoplastic composites. The heat transfer boundary conditions of the layup process are determined by establishing a mathematical model of the temperature field. The basic properties of the material are determined using CF/PEEK as the research object. The heat transfer parameters in the temperature field are analyzed to determine the thermal convection region affected by hot air and the radiated heat of the infrared lamp. And a finite element model of the temperature field is established. The FEM temperature field model was created to investigate heat transfer throughout the layup process, as well as the impact of mold heating, layup preheating, and varied heating temperatures on different layups. The temperature change law of different layups under different heating and preheating temperatures of hot air is analyzed; the online temperature measurement device is built. The experiment of automated fiber placement is carried out to analyze the heating performance of the infrared lamp and hot air gun and to determine their relevant parameters. Using the results of experiments and simulations, it has been determined that different mold temperatures are required for different layups; preheating can effectively reduce the temperature gradient between layups; and at a layup speed of 5 mm/s, a preheating temperature of 200 °C and a hot air temperature above 400 °C can ensure that the critical temperature between the prepreg wire bundle and layups reaches the melting point and they can be laid up normally.

Keywords Molding temperature · Molding quality · CF/PEEK · Carbon fiber reinforced thermoplastic composites · Finite element analysis

1 Introduction

The popularity of carbon fiber reinforced thermoplastic composites has exploded in recent years due to their superior performance in a wide range of industries. High-performance carbon fiber thermoplastic composites are used in cutting-edge aviation, aerospace, automotive, and marine manufacturing industries. Carbon fiber reinforced structures have been found to have good crashworthiness and the potential for significant weight reduction in automobile structural applications [1–4]. This material's features include outstanding inherent properties such as superior biocompatibility, better chemical resistance, high-temperature stability, and excellent mechanical properties [5–8]. According to Czaderski et al. [9] and Benedetti et al. [10] an accurate and uniform temperature is critical for achieving good mechanical characteristics. Sorrentino et al. [11] discovered exothermic peaks destroying interlaminar shear strength. To produce high-quality carbon fiber molded products, the control of the layup process becomes particularly important. Carbon fiber molded products of high quality have no bulging, no fractures, and a uniform thickness. Due to the temperature sensitivity of thermoplastic composites, it is necessary to investigate the temperature field in the process of AFP because the temperature will have different effects in different directions of the layup layer, which will ultimately affect the layup quality.

Currently, in the study of the temperature field of carbon fiber molding, more scholars are analyzing the distribution of the temperature field by establishing a mathematical model. By establishing a heat transfer model, the relevant

✉ Zhiqiang Liu
zhiqiangliu@just.edu.cn

[1] School of Mechanical Engineering, Jiangsu University of Science and Technology, Zhenjiang, China

conditions are determined according to the heating method and the environment, and most of the current analyses of the temperature field are performed with high-temperature gas heat sources. At present, in the study of the automatic layup process of thermoplastic composites, laser heating, infrared heating, and hot air heating have been applied to production, while ultrasonic welding, as an emerging heating method, has also been gradually applied to automatic layup and has become a hot spot in the study of thermoplastic composites.

Foreign countries are in the leading position in the related field due to advanced technology, and related studies on the temperature field started as early as around 2000. Fazil et al. [12] analyzed the crystallization behavior of composite materials under laser heating by establishing a heat transfer model to analyze the effect of temperature on the layup layer using a laser as the heat source. Stokes-Griffin [13] established a photothermal model using near-infrared heating to capture the anisotropic scattering behavior of the composites by the established photothermal model, and also investigated the effects of various source and surface models, and finally, the obtained experimental data and temperature variation curves reached a coincidence. A combined photothermal model established by Grouve [14] in order to optimize the process parameters, the light intensity distribution on the surface of the layup, and prepreg filament bundles was analyzed, thus predicting the heat distribution, and also investigating the effect of material properties and processing parameters on the temperature distribution produced.

Fredrik Lundström et al. [15] analyzed and calculated the temperature distribution between CFRP layups with different fiber contents in different directions by building a numerical model for the induction heating process. The final results were able to correspond to the numerical model through finite element analysis. Andreas et al. [16] used a laser as the heat source and proposed a new integrated analysis method to calculate the energy input of the laser based on geometric boundary conditions. The simulation study analyzed the distribution of the heat transferred from the laser to the prepreg tape in the mold and the press roll. In addition, the model has been optimized by the researchers concerned. Some scholars have analyzed the influence law of the temperature of the press roll on the temperature of the forming area during the layup process by establishing a two-dimensional finite element model related to the press roll [17].

This paper focuses on the analysis of the temperature field in the automatic layup process of carbon fiber reinforced thermoplastic composites. To determine the layup process in the temperature field, establish the heat transfer model of the temperature field and determine the boundary conditions; select the CF/PEEK material as the research object and determine its relevant physical properties; establish a three-dimensional model and determine the influence of temperature parameters on the layup layer during the layup process through finite element analysis. Through experimental analysis, we can determine the influence of preheating and heating on the layup through experimental analysis. The influence of the relevant temperature parameters on the temperature field under different parameters is analyzed.

2 Effect of temperature field on layup process

2.1 Brief description of carbon fiber automatic layup and molding process

The automatic layup technology of carbon fiber reinforced thermoplastic composites is that the prepreg filament bundle is transferred to the surface of the mold, melted and cured directly under the action of the heat source and the pressure roller, and molded by the action of the cooling device. The route of automated fiber placement in the temperature field of thermoplastic composites is shown in Fig. 1. According to the working principle of carbon fiber automatic layup, it

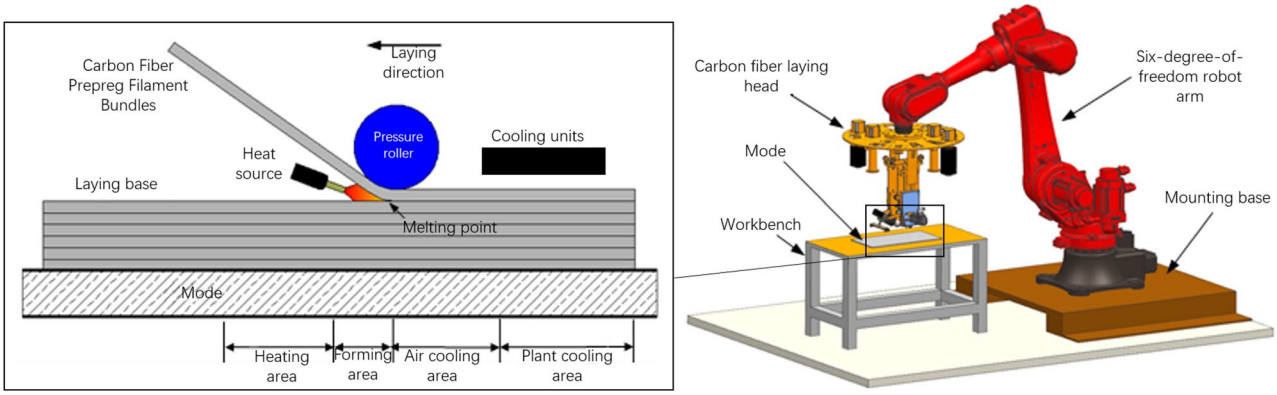

Fig. 1 Laying process route in temperature field

can be determined that the automatic layup area contains four, which are heating area, forming area, air cooling area, and device cooling area.

In Fig. 1, the role of the heat source is to heat the melt point between the prepreg wire bundle and the pavement base layer. The fluidity and viscosity of the resin matrix in the material increases, which makes the wire bundle obtain the necessary conditions for molding. The forming area is located behind the heating area. The prepreg bundle and layup base are molten in the forming area, and the resin matrix in the material flows, penetrates, and fuses together under the pressure of the press rollers. The cooling device cools down the fused pavement material to meet the requirement of crystallinity. In general, the cooling device is located at a certain distance from the forming area, resulting in an air cooling zone between the two areas; this zone is adjusted according to the processing requirements, etc.

Thermoplastic composites have high-temperature requirements. In addition to the conventional heating zone in the fiber layup process, the molding process should also contain a preheating zone, whose main function is to increase the temperature of the base layer, thus reducing the heating time in the main heating zone and improving the layup efficiency. The specific effect of preheating on the layup substrate needs to be determined by relevant simulation and experimental analysis.

The melting temperature of carbon fiber reinforced thermoplastic composites is about 340 °C. At the same time, carbon fiber reinforced thermoplastic materials have high-temperature requirements, so the selection of a heat source becomes very important. Currently, the most commonly used heat sources are laser, heat gun, and infrared lamp. Laser heating has been the core heat source for the study of thermoplastic composites in recent years. It has the highest heat transfer efficiency and is easy to control, but is expensive; infrared heating has a wide range of radiation, but cannot focus on heating the molding area; hot air heating has a concentrated range and has some advantages that laser heating has not, so hot air heating is chosen as the heat source for this paper. At the same time, the influence of carbon fiber preheating is considered, and the infrared lamp is used as the preheating heat source.

2.2 Mathematical model of the temperature field during the automatic placement of carbon fiber

By understanding the thermoplastic composite automatic layup temperature field layup process, the prepreg wire bundle is placed on the mold and the layup base by the heat source and the pressure of the pressure roller to realize the composite automatic layup molding. The whole layup process is carried out in three-dimensional space, and the relationship between the prepreg bundle, the layup base, and the heat source needs to be considered. However, in the actual layup process, considering that the hot air has an influence beyond the prepreg bundle and the layup base when heating the layup and the mold, it is assumed in the study that the heat is uniform in the width direction when it is transferred into the prepreg bundle. By using the law of conservation of energy, the heat transfer model of the filament bundle in the horizontal and vertical directions is established, and the heat transfer equation [18] is formulated as follows.

$$\rho c\frac{\partial T}{\partial t} = k_1 \cdot \frac{\partial}{\partial x}\left(\frac{\partial T}{\partial x}\right) + k_2 \cdot \frac{\partial}{\partial y}\left(\frac{\partial T}{\partial y}\right) \tag{1}$$

ρ denotes the density of the carbon fiber prepreg tow, c denotes the specific heat capacity of the carbon fiber prepreg tow, k_1 denotes the thermal conductivity in the x-direction, k_2 denotes the thermal conductivity in the y-direction, and t is time. k_1 and k_2 are considered constant. In addition to the physical quantities affected by the temperature field expressed in Eq. 1, heat is also generated inside the prepreg tow, but the effect on the whole automatic layup forming process is small compared to that of the heat source and can therefore be neglected.

The carbon fiber automatic layup process uses a continuous and uniform unidirectional prepreg tow. Due to the anisotropy of the carbon fiber material, the heat conduction is relatively uniform in the width direction of the prepreg tow, but the heat conduction of the prepreg tow along the layup direction and the vertical direction of the layup layer has a large deviation, so the effect of heat transfer in the width direction is ignored. According to the law of thermodynamics, a two-dimensional heat transfer model is established along the direction of filament bundle conduction and the thickness direction of the layup layer [19].

2.2.1 Temperature field geometry model

The two-dimensional heat transfer model of the automatic layup molding process of carbon fiber reinforced thermoplastic composites is shown in Fig. 2. In addition to the effect of heating on the prepreg wire bundle and the layup base layer, the analysis of the mold and the pressure roller were added to the heat transfer mathematical model to fully consider the heat transfer between the layup and the mold, and between the mold and the prepreg wire bundle. Information on the location parameters, transfer boundaries, and etc. between each object was determined. Instead of assigning velocities to the entire control volume, a simulation of continuous layup is used in the analysis of the entire forming process, where the prepreg wire bundle is formed in one whole layup.

In the heat transfer model, the direction of prepreg wire bundle layup is horizontal to the left and the velocity is set

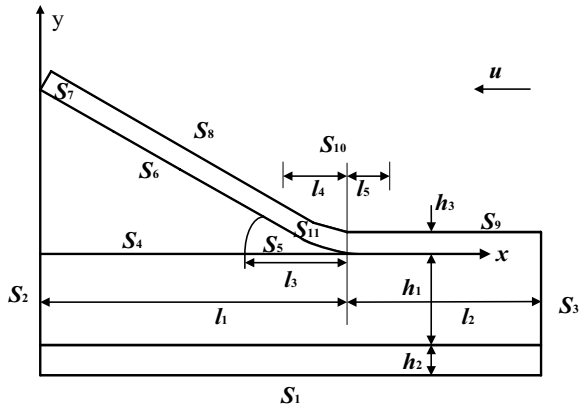

Fig. 2 Heat transfer model of temperature field

to u. The positive direction of the x-axis is opposite to the direction of layup forming and is horizontal to the right; the y-direction is vertical up along the layup direction and is located on the leftmost side. After the coordinate system is fixed, it will not change because of the thickness of the layup base and the change of the melt forming point. In the figure, S indicates the individual faces in the temperature field. h_1 and h_2 indicate the height of the layup layer and the mold, respectively. h_3 indicates the thickness of the single prepreg bundle, and l_1 indicates the horizontal distance between the melt point and the origin. l_2 indicates the distance between the melt point and the layup start point. l_3 indicates the length of the direct heating area. l_4 and l_5 indicate the horizontal contact length between the nip roll and the laid-up prepreg bundle. It depends on the roll diameter, roll pressure [20], and laying angle. In the actual forming process, the x-coordinate of the forming melt point does not coincide with the center of the press roll because the layup base and the prepreg bundle are deformed by the pressure [21].

2.2.2 Boundary conditions

In order to solve the heat transfer equation, it is necessary to determine the boundary conditions of the temperature field, first assuming that the surface temperatures of the mold and the layup are T_a and T_b, respectively. At the time when the layup has not started (time $t=0$),

S_1, S_2, and S_3 are the faces of the mold surface, and the temperatures of the three surfaces satisfy $T=T_a$:

S_6, S_7, and S_8 are the surfaces of the prepreg wire bundle, and the temperatures of the three surfaces satisfy $T=T_b$:

After the start of auto-layout, the hot air affects the temperature field with the following boundary conditions according to Fourier's law as well as Newton's cooling equation:

S_4 is the pavement base surface and S_9 is the completed pavement of the prepreg wire bundle pavement, with both surfaces satisfying:

$$-k_m\frac{\partial T(x,y)}{\partial m}=h_1(T-T_z) \tag{2}$$

m denotes the normal direction of the heat transfer surface, h_1 is the heat transfer coefficient of the prepreg wire bundle surface under natural convection, and T_Z is the ambient temperature.

On S_4, x and y satisfy, respectively: $0 \le x \le l_1 - l_4$, $y = h_1 + h_2 + h_3$;

On S_9, x and y satisfy, respectively: $l_2 + l_3 \le x \le l_1 + l_4, y = h_1 + h_2$.

Also, considering that the heat transfer coefficient of the pressure roller is relatively large compared to the prepreg wire bundle because of the difference in the material in the automatic laying equipment, we use the pressure roller for direct cooling during the laying process.

On the S_{10} side, satisfying

$$-k_m\frac{\partial T(x,y)}{\partial m}=h_s(T-T_s) \tag{3}$$

h_s is the convective heat transfer coefficient of the press roll, T_s is the surface temperature of the press roll in the process of laying, and x and y satisfy $l_2 - l_5 \le x \le l_2 + l_4$, $y = h_1 + h_2 + h_3$;

On the mold faces, S_1, S_2, S_3, satisfying:

$$-k_m\frac{\partial T(x,y)}{\partial m}=h_r(T-T_r) \tag{4}$$

h_r is the convective heat transfer coefficient of the mold; T_r is the surface temperature of the mold during layup:

On S_1, x and y satisfy $0 \le x \le l_2 + l_1, y = 0$

On S_2, x and y satisfy $x = l_1 + l_2, 0 \le y \le h_2$;

On S_3, x and y satisfy $x = 0, 0 \le y \le h_2$

On faces S_5 and S_{11}, meet:

$$-k_m\frac{\partial T(x,y)}{\partial m}=h_n(T-T_a) \tag{5}$$

h_n is the heat transfer coefficient of the prepreg wire bundle under forced convection conditions; T_a is the temperature generated by the heating of the infrared lamp in the laying process; x and y satisfy $l_2 \le x \le l_2 + l_3, y = h_1 + h_2$

2.2.3 Determination of model input parameters

The relevant parameters in the mathematical model of the temperature field are shown in Table 1.

Table 1 Parameters of temperature field mathematical model

Parameter	Unit	Value
Thickness of prepreg wire bundle h_3	mm	0.15
Width of prepreg wire bundle d_2	mm	6
Length of prepreg wire bundle l	mm	250
Thickness of pavement base h_2	mm	3.2
Number of pavement layers n	Layer	6
Thickness of the mold h_1	mm	10
Radius of pressure roller r	mm	30
Length of prepreg wire bundle before contact with press roll l_1	mm	10
Length of prepreg wire bundle after contact with press roll l_2	mm	4
Thermal conductivity of the mold	W/mm^2.℃	45
Temperature of hot air T_0	℃	350–500
Temperature of the environment T_z	℃	25

2.3 Basic physical properties of carbon fiber reinforced polyetheretherketone composites

2.3.1 Material property parameters

The carbon dimension reinforced polyether ether ketone composite (CF/PEEK) selected for this paper was carried out. The CF/PEEK composite is made from carbon fibers impregnated with a thermoplastic resin matrix polyether ether ketone, which is an intermediate material for creating thermoplastic carbon fiber products. The CF/PEEK has excellent thermal stability and can maintain good mechanical properties [22] under high-temperature conditions. The relevant physical parameters of the CF/PEEK material are shown in Table 2.

The mold selected for this experiment is made of common 45 steel, and the parameter properties of the material are shown in Table 3.

The CF/PEEK prepreg is shown in Fig. 3.

Table 2 CF/PEEK-related parameters

Parameter	Value
Capacity for specific heat C (J/kg·℃)	1425
Density ρ (kg/m^2)	1560
Temperature at which something melts T_r (℃)	343
Thermal conductivity in the X-direction K_x (W/m^2℃)	6
Thermal conductivity in the Y-direction K_y (W/m^2℃)	0.72
Width d (mm)	6
Thickness h_3 (mm)	0.15

Table 3 Mold physical parameters

Parameter	Value
Capacity for specific heat C (J/kg·℃)	470
Density ρ (kg/m^2)	7800
Thermal conductivity K (W/m^2℃)	45

2.3.2 Material heat parameter change curve

The basic properties of carbon fiber reinforced polyether ether ketone composites (CF/PEEK) were introduced previously. The resin matrix polyether ether ketone has excellent thermal stability but is relatively difficult to process and mold, with a melt temperature of 343 °C. Moreover, basic physical properties such as the degree of deformation are highly susceptible to temperature, and the variation is not linear [19]. The natural deformation temperature profile of carbon fiber reinforced polyetheretherketone thermoplastic composites (CF/PEEK) subjected to heat is shown in Fig. 4.

At the beginning, the material is tightened until it reaches the melting point, i.e., the deformation is negative because the increase in temperature leads to the thermal expansion of the composite, and near the melting point of 340 °C, the deformation of the composite starts to increase to a positive value, and the final natural deformation is maintained at about 0.2 mm.

In addition to the temperature affecting the deformation of the material, the related parameters such as specific heat capacity and thermal conductivity of polyether ether ketone are also affected by the temperature. The temperature variation curves of the two parameters are shown in Figs. 5

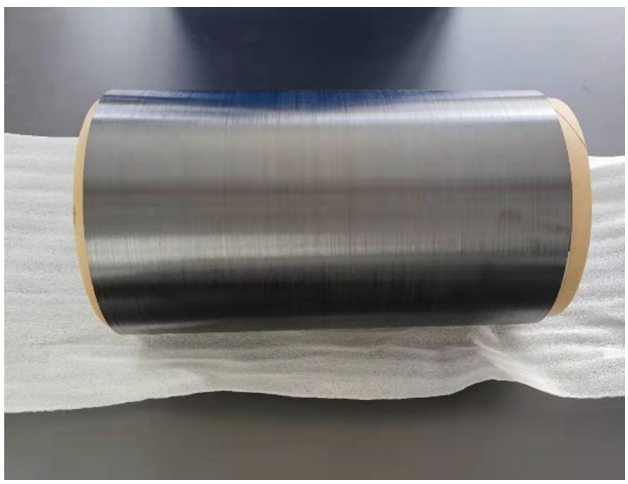

Fig. 3 CF/PEEK prepreg

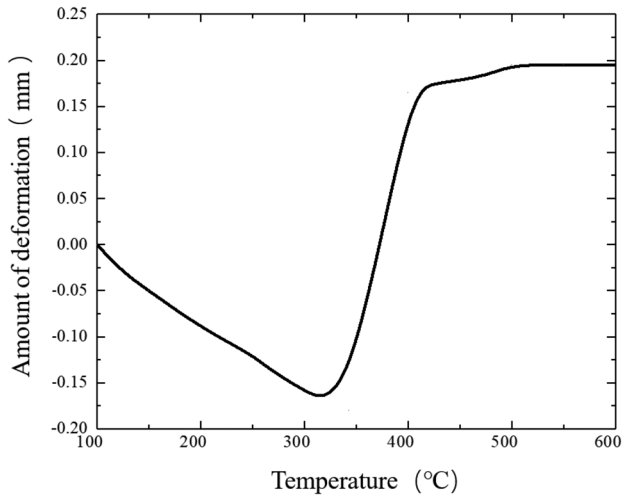

Fig. 4 Thermal deformation curve of CF/PEEK

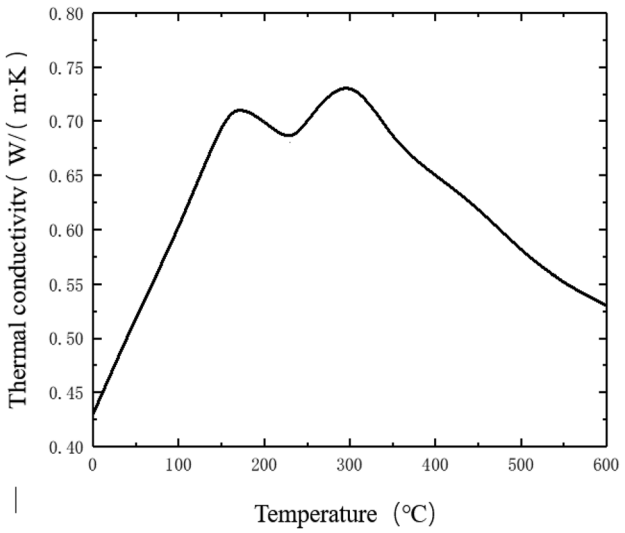

Fig. 6 Thermal conductivity of CF/PEEK

and 6. According to the curves of the two parameters, the specific heat capacity of carbon fiber polyetheretherketone reinforced composites is proportional to the temperature, and the thermal conductivity will fluctuate and change at several critical points of 150 °C, 230 °C, and 340 °C. The thermal conductivity will gradually decrease when the melting point is reached.

2.3.3 Thermal weight analysis

The CF/PEEK resin matrix is PEEK, and the resin needs to take into account its thermal decomposition temperature during the heating process, so when considering the heating temperature, the temperature limit should be fully considered, so the thermogravimetric analysis was performed, and a thermogravimetric analyzer (TG209F3, NETZSCH, Germany) (Fig. 7) was selected for the thermogravimetric analysis, and the experiment-related parameters are shown in Table 4.

The TGA curve of CF/PEEK obtained after the test is shown in Fig. 8.

According to the curve, it can be seen that the thermal decomposition of PEEK starts at 540.2 °C and the maximum decomposition temperature is 585.1 °C. Therefore, this can be used as a reference for heating, and the influence of the decomposition temperature needs to be considered to control the temperature of the molding point within a suitable range.

2.4 Heat transfer parameters of the temperature field

In the automatic layup process, the hot air gun, as the heat source, is moving with the layup head of the forming device, and the hot air is sprayed through the nozzle to heat the material, affecting the convection boundary conditions on

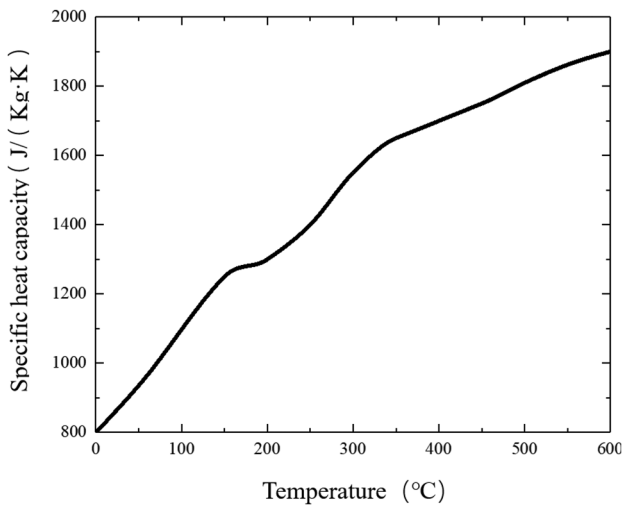

Fig. 5 CF/PEEK specific heat capacity

Fig. 7 Thermogravimetric analyzer

Table 4 Experimental parameters

Parameters of the condition	Values of parameters
Temperature of the test	20–800 ℃
Heating rate	10 K/min
Atmosphere	N_2

the prepreg wire bundle so that it changes with the change of position of the thermal load. The convection zone is divided into two cases: The first one is the forced convection heat transfer zone, when the prepreg wire bundle is directly heated by the direct blowing of the hot air gun; the other one is the natural convection heat transfer zone, when the prepreg wire bundle in this zone is not directly heated, so the convection transfer coefficients of different zones need to be considered during the thermal analysis.

Additionally to heat convection, thermal radiation is a form of heat transfer. During the heating process, the material will gradually emit thermal radiation into the surrounding environment; the infrared lamp will be used as a preheat; and the infrared lamp will be heated in a way that is also thermal radiation. This section analyzes the thermal convection and thermal radiation parameters in the temperature field during the heat transfer process.

2.4.1 Natural convection heat transfer coefficient of temperature field

When the pavement is in a region without direct heating by hot air, a natural convection region is generated by the air flow, although not driven by hot air. Within the natural convection zone, the relevant parameters are determined by the characteristic temperature *tb*, which is calculated by the formula:

$$t_b = \frac{t_f + t_v}{2} \tag{6}$$

t_f is the convective heat transfer surface temperature; t_v is the temperature of the fluid.

The equation for the heat transfer coefficient h_1 of the natural convection heat transfer surface is shown below:

$$h_1 = \frac{k_b}{l_f} Nu_b \tag{7}$$

Nu_b is the Nusser number, k_b is the thermal conductivity, and l_f is the length of the natural convection region. When performing convective heat transfer calculations, the natural convection criterion in space is studied and the Nusser number is calculated, satisfying the following relation.

$$Nu_b = P(Gr \cdot Pr)^Q \tag{8}$$

Gr is the Glachov number, Pr is the Air Plante number, and P and Q are two coefficients, which are jointly determined by the Glachov and Plante numbers.

The Glachov number determines the form of natural convection flow and is calculated as

$$Gr = \frac{g\sigma t_k l_z}{v^2} \tag{9}$$

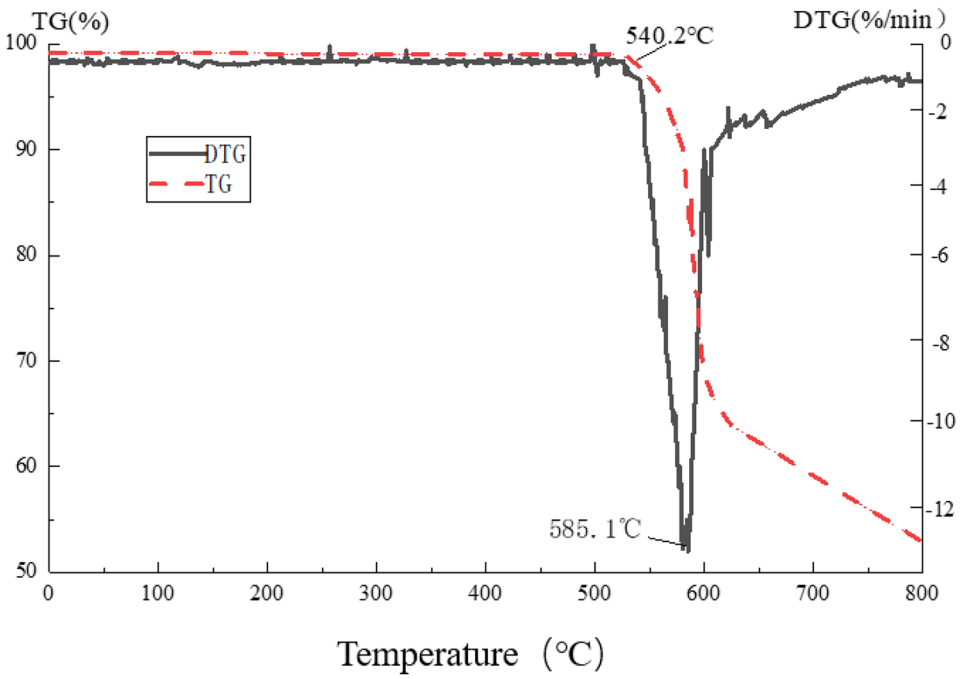

Fig. 8 TGA change curve of CF/PEEK composite material

g denotes gravity's acceleration; σ denotes the expansion coefficient of volume, taking the value determined by tb; tk denotes the temperature difference between the convective heat transfer surface temperature and the air temperature, and lz denotes the size of the natural convection zone; and v denotes the viscosity coefficient of air.

$2 \times 10^4 < Gr \cdot Pr < 8 \times 10^6$, the Nusser factor is calculated as:

$$Nu_b = 0.54(Gr \cdot Pr)^{1/4} \tag{10}$$

When $8 \times 10^6 < Gr \cdot Pr < 10^{11}$, the Nusser factor is calculated as:

$$Nu_b = 0.15(Gr \cdot Pr)^{1/3} \tag{11}$$

The natural convection heat transfer coefficient curve up to 300 °C is calculated and shown in Fig. 9.

2.4.2 Temperature field forced convection heat transfer coefficient

In the automatic laydown, the area directly affected by the hot air is the forced convection conduction area, at this time directly affected by the surface S_5 and S_{11}, following the viscous force similarity criterion (Reynolds criterion), that is, at this time the surface heat transfer satisfies Eq. 12

$$Re = \frac{l_q \cdot u_v}{v} \tag{12}$$

Re is the Reynolds number, l_q is the length of the forced convection region, u_v is the flow rate of hot gas generated by the heat source in the forced convection region, and v is the viscosity of the hot gas dynamics. In the viscous force similarity criterion, the Reynolds number of is taken to have different values. The Nurse criterion Nu_b satisfies two cases.

When $Re > 5 \times 10^5$, the Nusser factor is calculated as:

$$Nu_b = 0.66Pr^{1/3}Re^{1/2} \tag{13}$$

When $5 \times 10^5 < Re < 10^7$, the Nusser factor is calculated as:

$$Nu_b = Pr^{1/3}(0.037Re^{4/5} - 871) \tag{14}$$

According to the boundary temperature calculation formula and the natural convection heat transfer coefficient formula, the hot gas flow rate of 6.5 m/s is selected, and the forced convection heat transfer coefficient is obtained by calculation at different temperatures as shown in Fig. 10. When the temperature is between 300 and 600 °C, the strong convection heat transfer coefficient of thermoplastic composites is maintained at about 65 W/m^2℃ in the temperature field, and the change is small in the temperature interval, which keeps a stable up state.

2.4.3 Thermal radiation of the temperature field

In this paper, the choice is infrared lamps for preheating. The preheating temperature should not be kept at about 200 ℃ which is commonly used. The use of a hot air gun as a preheating heat source will complicate the mechanism because hot air can only be used for a limited range of heating. Infrared heat sources are radiation range heating and can have a better preheating effect.

In the temperature field, the radiation heat generated by the infrared lamp is unevenly distributed along the layering direction according to Stefan's law of thermodynamics.

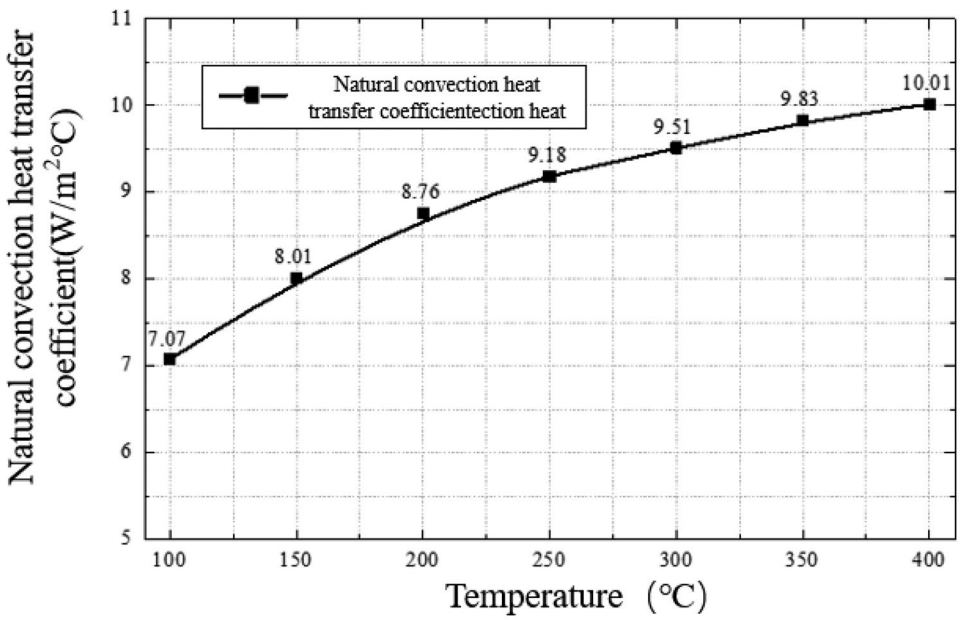

Fig. 9 Heat transfer curve of natural convection

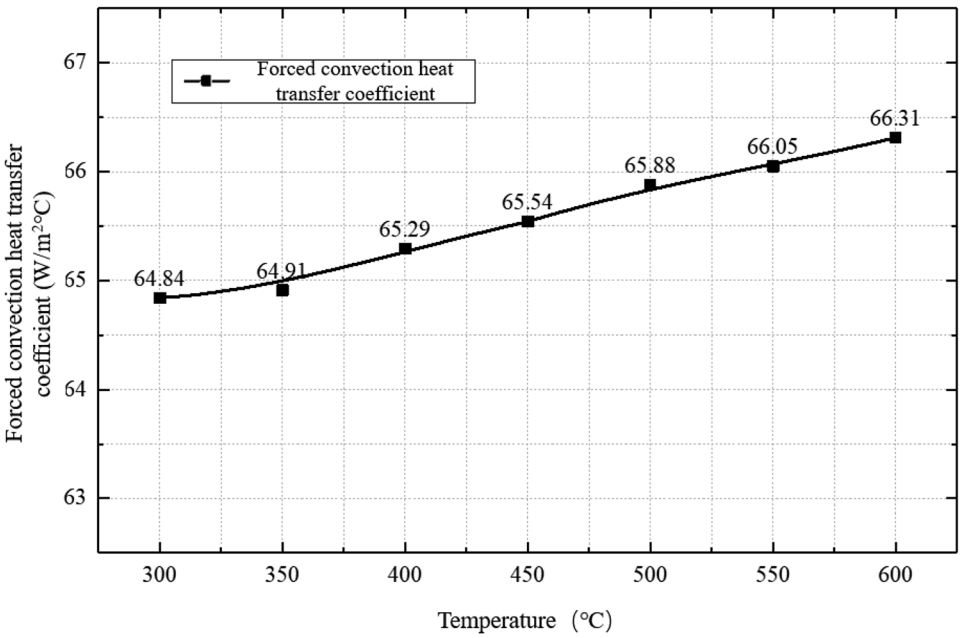

Fig. 10 Forced convection heat transfer curve

$$G = \sigma \varepsilon T_d^4 \tag{15}$$

G is the radiation intensity of the infrared lamp; $\sigma = 5.67 \times 10^{-8} W \cdot m^{-2} \cdot K^{-4}$ is the Stephan constant; ε is the radiation coefficient; T_d is the lamp generation temperature. The radiation intensity of the lamp can be obtained according to the heating power P by the infrared lamp, satisfying the formula

$$G = \frac{P}{A} \tag{16}$$

A is the radiating area of the lamp, because the lamp filament is spirally wound and satisfies the formula:

$$A = 2\pi \delta RL \tag{17}$$

δ is the spiral density coefficient of the lamp filament, R is the radius of the lamp, and L is the length of the lamp. Substitution gives the formula.

$$G = \frac{P}{2\pi \delta RL} \tag{18}$$

Therefore, the radiation intensity of the lamp can be controlled by adjusting the lamp power.

2.5 Temperature field finite element simulation analysis

In this section, the thermodynamic simulation module of Workbench is used to simulate and analyze the temperature field of the model, to simplify the model, and to analyze the changes produced by the model in the temperature field under different conditions.

In the previous section, we described the workflow of the carbon fiber forming equipment in the temperature field. During the layup process, the heat source moves with the carbon fiber forming equipment, which causes the temperature in the temperature field to change, so it cannot be analyzed by steady-state heat. Therefore, the thermal module in the Workbench is chosen to perform transient thermal analysis of the temperature field. The transient thermal analysis is divided into three main parts: preprocessing, solution, and post-processing, which are used to analyze the loads at different nodes that change with time. The preprocessing module defines the analysis unit, imports the completed UG modeling model, and sets the basic material parameters; the solving module sets the basic load parameters; the post-processing module analyzes the transformed temperature cloud and change curve to grasp the simulation law; and the preprocessing model is shown in Fig. 11.

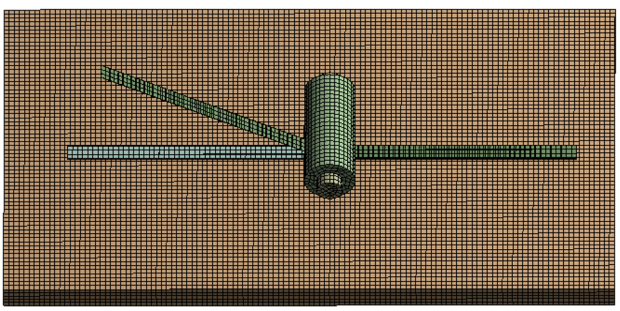

Fig. 11 Preprocessing generation model

2.5.1 Finite element transient heat transfer equation

After determining the model, the differential equation for thermal conductivity of the temperature field is transformed into an implicit transient heat transfer equation in order to cover the temperature dependence of the material parameters and to follow the general energy conservation law.

$$\left[C_P\right]\left\{T_t\right\} = \{P\} - [H]T_i \tag{19}$$

$[C_p]$ is the specific heat matrix considering the internal energy variation of the system, $\left\{T_t\right\}$ is the derivative of the node temperature with respect to time, $\{P\}$ is the node heat flow rate vector, $[H]$ is the heat conduction matrix considering convection and thermal conductivity, and T_i is the node temperature vector. By simulating the input data, the analytical data on the temperature variation of the pavement in the temperature field with different temperature parameters is obtained.

2.5.2 Effect of mold and preheating on temperature field

(1) The effect of mold temperature on first layer layup

Most of the studies in the analysis of the temperature field simulation results ignore the influence of the mold on the temperature field. The whole layup process is carried out on the mold, and there is a large temperature gradient between the mold and the first layup layer. If the mold temperature is not high enough, it will lead to the reduction of the bond between the first layup layer and the silk bundle, and it cannot be laid up properly, so the influence of the mold temperature needs to be considered. In this paper, the influence of preheating on the layup of the first layup layer is analyzed, and the influence curve is shown in Fig. 12.

A total of 400 °C, 450 °C, and 500 °C were selected to study the effect of preheating on the first pavement layer, and the preheating temperature was set in the range of 20–200 °C. The hot air is heated at two different temperatures, and the overall trend of temperature change of the first pavement layer is similar at different preheating temperatures. It can be seen that when the hot air temperature is 500 ℃, the mold heating temperature needs to go to 260 ℃ to ensure that the first layer of pavement temperature reaches the critical temperature, and when the hot air temperature is 450 ℃, it also needs to control the mold temperature above 300 ℃ to ensure that the first layer of pavement temperature reaches the critical temperature. According to the trend of temperature change, when the hot air temperature decreases by 50 ℃, the mold temperature needs to increase by 20 ℃ to meet the first layer layup requirement. Therefore, when the first layer is laid, the mold temperature should be heated to 260 °C, the

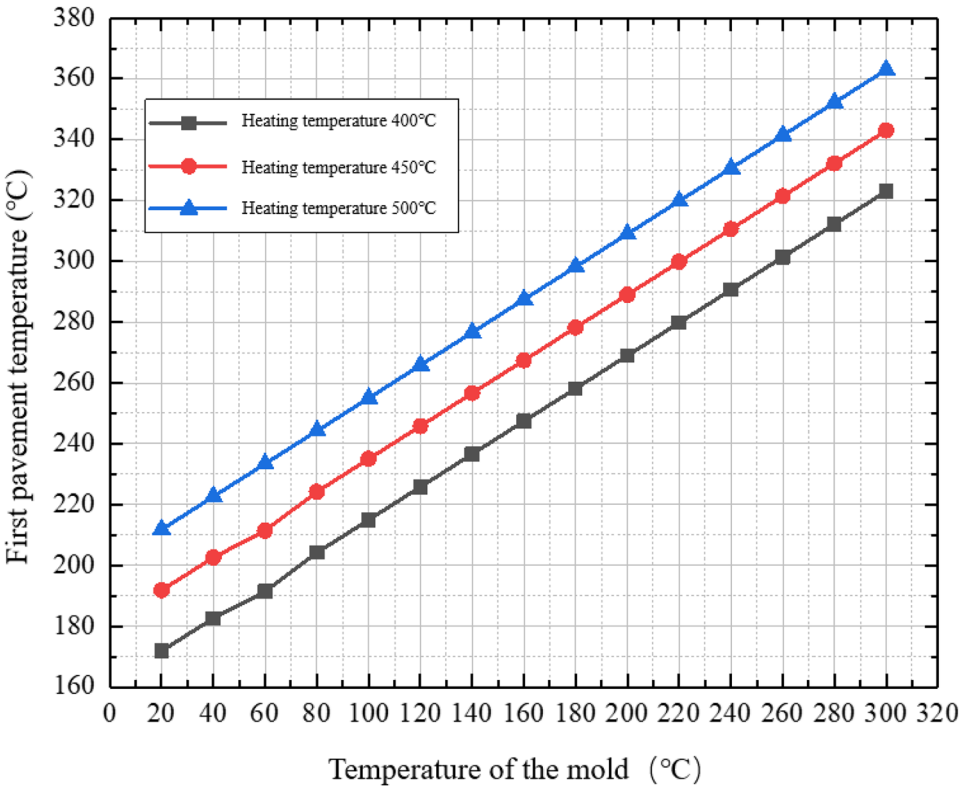

Fig. 12 The influence of preheating temperature on paving

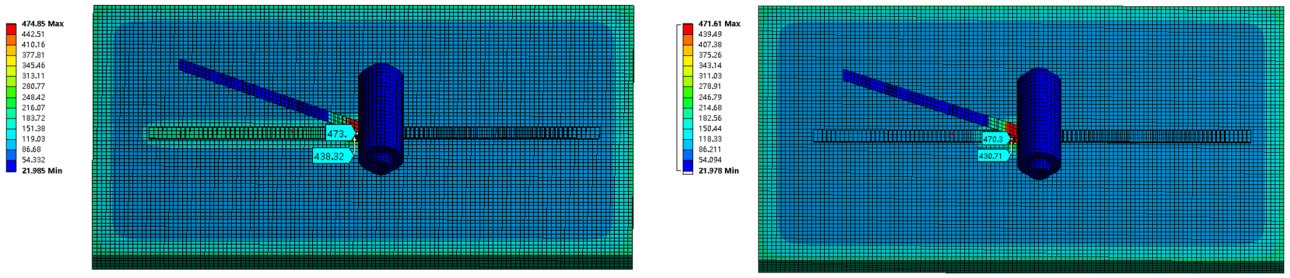

Fig. 13 Laminate preheating temperature cloud map

normal melting of the first layup layer. However, the glass transition temperature of PEEK prepreg is 143 °C. Keeping the temperature above the glass transition temperature for a long time will lead to a decrease in the crystallinity of the filament bundle, so the method of variable process preheating is used, and the mold temperature needs to be set at 140 °C when the other layers are laid up. When the crystallinity of the carbon fiber product is reduced, bulging may occur and result in incomplete compaction between the layup layers, affecting the life and mechanical properties of the carbon fiber product.

(2) Effect of preheating on layup

There are many methods and types of preheating. The most commonly used is the preheating of the mold, but as the number of layers laid increases, the influence of the mold will gradually diminish. Therefore, preheating can be done by adding preheat externally. In the simulation, the influence of the preheating method on the layup layer is ignored, and the preheating target temperature is directly set for the layup layer in the simulation, and the influence of different preheating temperatures on the temperature field distribution state of the layup base layer is analyzed, and then its influence on the molding is analyzed.

During the layup process, the pavement layer directly affected by temperature is the pavement layer in contact with the prepreg wire bundle. The number of pavement base layer is six. The sixth pavement layer and prepreg wire bundle contact molding is the pavement base layer most likely to decompose, but the fifth layer at the same time will be more affected by the heating process. The temperature gradient between different pavement layers will affect the molding effect, as shown in Fig. 13.

The same cross section was taken and the temperature difference between the layered surfaces was compared for the two working conditions. As shown in Table 5, the temperature variation between the two layers with and without preheating is compared.

By comparing the temperature change of preheated 200 °C and unpreheated pavement, the temperature of the sixth and fifth plies was significantly increased under the influence of preheated temperature, and the temperature difference between plies was reduced by 4.92 °C compared with that of unpreheated, implying that preheating can reduce the temperature gradient between plies more effectively and improve the molding effect.

Table 5 The influence of preheating on paving

Preheating situation	Temperature of the 6th floor (°C)	Temperature of the 5th floor (°C)	Temperature differences (°C)
No preheating	470.3	430.7	39.6
Preheating 200 ℃	473	438.32	34.68

2.5.3 Effect of the number of layers on the temperature field

In the actual layup process, the effect of temperature on the layup layers varies non-linearly among each other, so it is necessary to study the law of heat change of different layup

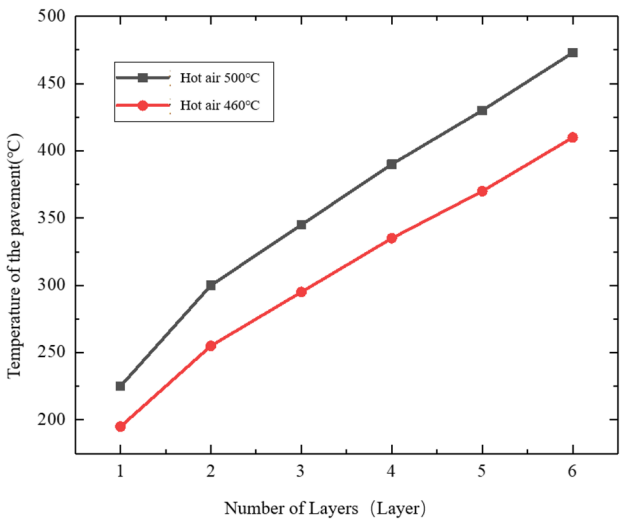

Fig. 14 Curves of different layers affected by temperature

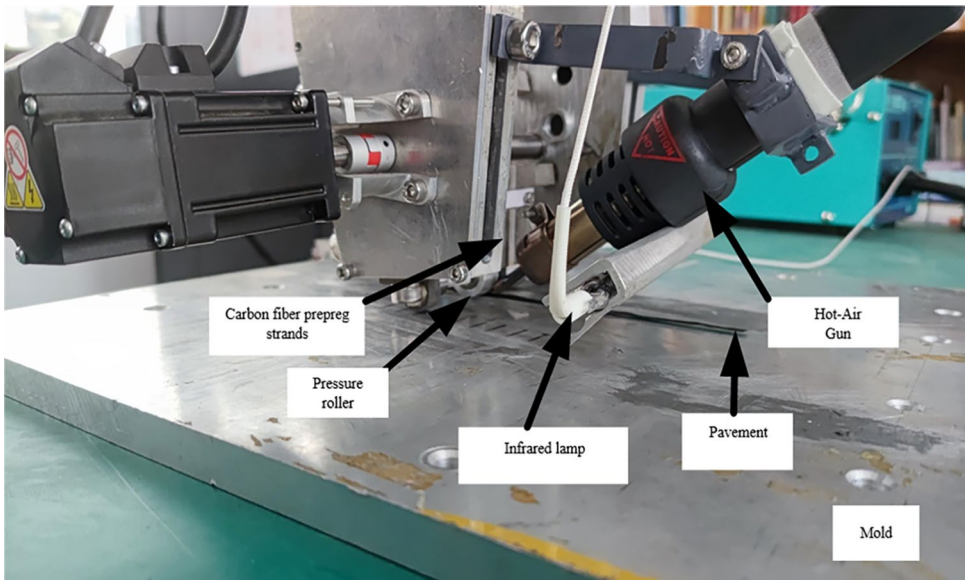

Fig. 15 Experimental setup diagram

layers under different temperatures. In the simulation, the effect of preheating is considered. The mold temperature is kept at 140 ℃, a preheating temperature of 200 ℃ is used, and the temperature of hot air is set to 500 ℃. There are six layers of layup base in the temperature field, and the temperature change of six different layup layers is analyzed when the seventh layer of layup is carried out, and the change curve is shown in Fig. 14.

According to the curve, it can be seen that the hot air temperature of 460 ℃ and 500 ℃ heats the pavement layer in the upper pavement layer because the hot air temperature is larger and the temperature effect of the pavement layer is smaller, which makes the temperature difference of the pavement layer close to the actual hot air temperature difference when the two sets of heating temperatures heat the pavement layer under the same pavement layer; when the

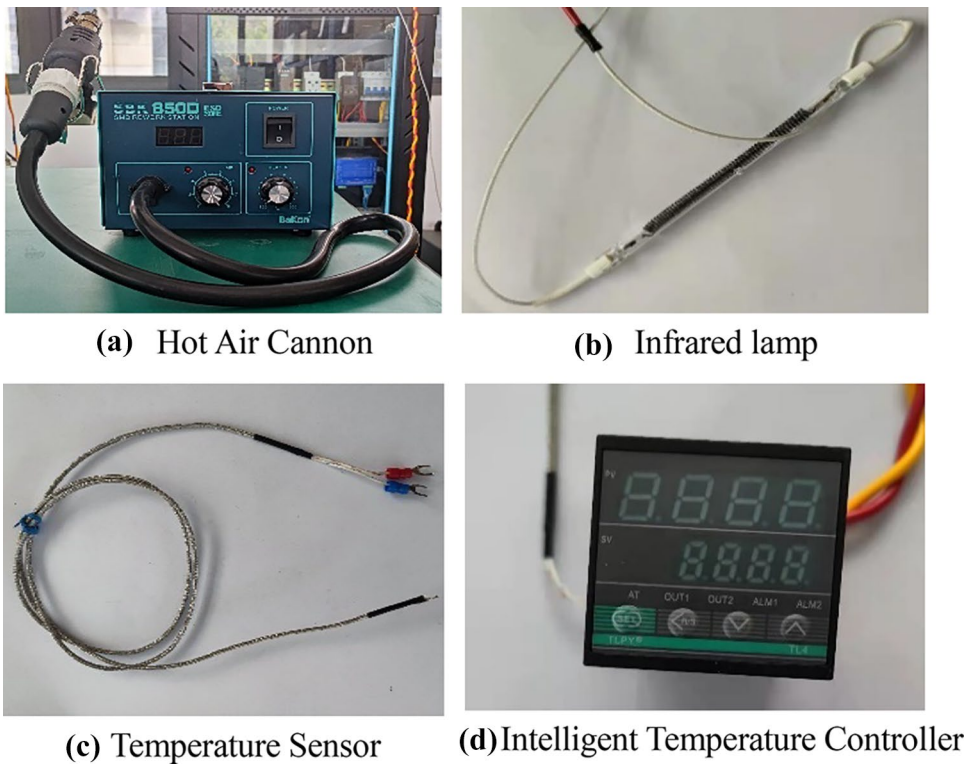

Fig. 16 Temperature field experimental device

Table 6 Related parameters of infrared tube

Parameter	Values/models
Rated voltage	220 V
Material	Spiral carbon wires
Length	18 mm
Maximum heating temperature	400 ℃
Quantity	2

pavement layer is closer to the mold, the influence of the mold temperature increases and the influence of the hot air decreases, which leads to the decrease of the temperature difference of the pavement layer heated by the two heating.

According to the results of the simulation, the mold is heated at a variable temperature, and when the first layer is laid, the mold heating temperature is 260 ℃; when the other layers are laid, the mold temperature is set to 140 ℃. The preheating temperature of the high paving layer is set to 200 ℃, and the parameters related to the hot air temperature need to be determined by experiment.

2.6 Temperature field automatic laydown temperature influence experiment

In order to verify the results of the finite element analysis and to determine the relevant parameters, an online temperature measurement device needs to be built to determine the temperature changes of different layers in different directions in the temperature field and also to determine the influence of the preheating temperature on the carbon fiber layup according to the temperature measurement device. The temperature measurement device is mainly composed of a temperature sensor and an intelligent temperature controller. The front end of the temperature sensor is connected to the pavement, and the other end is connected to the intelligent temperature controller, which can monitor the temperature change in real time through the collected temperature sensor signal.

The physical diagram of the experimental setup related to the temperature field is shown in Fig. 15. In this paper,

Table 7 Related parameters of hot air gun

Parameter	Value/model
Rated power	550 W
Air flow rate	22 L/min
Temperature range	100–500 ℃
Temperature stability	± 1 ℃
Air outlet device	Air-pump type
Air outlet diameter	6 mm
Input voltage	220–240 V

Table 8 Related parameters of intelligent temperature controller

Parameter	Value/model
Rated voltage	220 V
Temperature measurement range	0–1300 ℃
Division number	K
Temperature response time	1 S

six to seven groups of temperature sensors were selected for the analysis of different pavement layers and the same pavement level. A staggered arrangement of temperature sensors for different pavement levels is used because it can reduce the influence on the temperature generated in the pavement thickness direction. Figure 16 shows a physical display of the main equipment used in our experiments.

2.6.1 Choice of experimental setup

The basic properties of the material chosen for the experiments, CF/PEEK, are described in the previous section and will not be repeated here. The main device needed to conduct the experiments consists of infrared quartz heating tubes, as shown in Table 6.

The relevant parameters of the industrial heat gun are shown in Table 7.

The relevant parameters of the intelligent temperature controller are shown in Table 8.

Thermocouple temperature sensor-related parameters are shown in Table 9.

The sensor arrangement is shown in Fig. 17. Because the width of the prepreg wire bundle is smaller than the sensor length, the edge of the sensor is fixed by high-temperature insulation tape, which can effectively prevent the residual heat of the air outlet from affecting the sensor temperature measurement during the heating process.

2.6.2 Preheating experiment of infrared lamp

The preheating experiment was mainly to analyze the influence of the infrared lamp on the layup. The heat generated by the preheating of the infrared lamp on the temperature field was mainly irradiation heat, and first, the carbon fiber layup was analyzed without considering the heating of the

Table 9 Related parameters of thermocouple temperature sensor

Parameter	Value/model
Model	K
Temperature range	0–600 ℃
Type	Exposed
Diameter of temperature measuring head	1 mm
Number	7

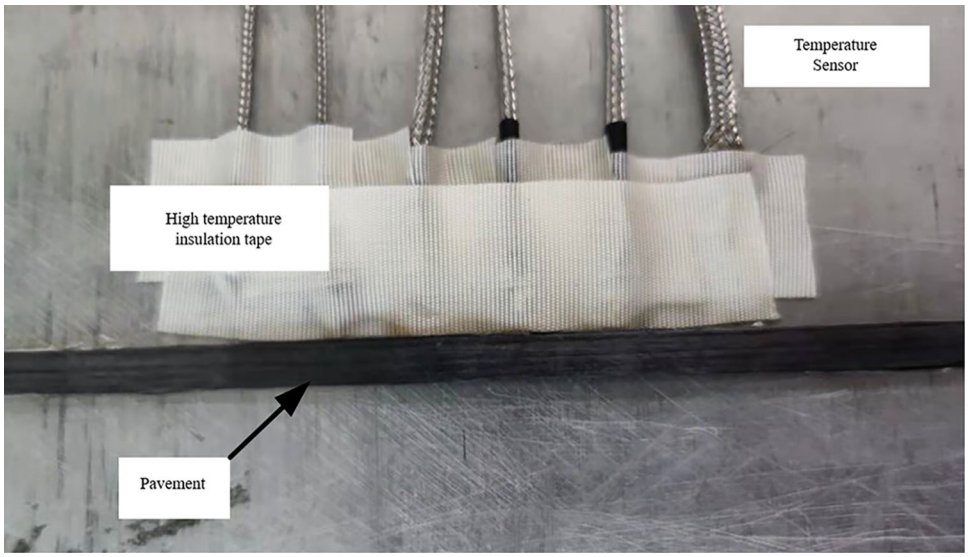

Fig. 17 Sensor layout diagram

heat gun. The temperature change of the temperature sensors at different heights from the mold was analyzed by arranging six groups of temperature sensors horizontally on the pavement surface at 20 mm intervals without paving to determine the influence range in the temperature field, and the principle of the temperature measurement device is shown in Fig. 18.

The temperature change curve collected through the experiment is shown in Fig. 19. This experiment selected three preheating temperatures of 300 ℃, 250 ℃, and 200 ℃ for analysis. The pavement was heated by various temperatures. When the heating temperature was 300 °C, the highest temperature measured directly below the heat source by temperature sensor #4 was 253 °C at a preheated heat source height of 10 mm. With the distance increasing, the temperature gradually decreases, but the temperature drop is large, at the distance of 30 mm from the lamp no. 1 temperature sensor to collect the temperature of only 141 ℃.

In the 300 ℃ and 200 ℃ heating under the influence of distance, the overall temperature change trend is the same, but the lower the heating temperature, with the increase in temperature measurement distance, the temperature difference gradually becomes larger. It can be seen that the infrared heating radiation ranges of about 40 mm, so this paper considers the use of multiple groups of lamp combinations by expanding the radiation range and then improving the efficiency of preheating. The experiments chose two groups of infrared lamps side by side for preheating, resulting in six measurement points of temperature sensor peak temperature change as shown in Fig. 20.

The shaded bar graph in the figure shows the temperature change curve after the double lamp. By comparing the temperature curve collected by the single lamp under the same temperature, the double lamp design has a significant increase in temperature relative to the single lamp. Taking 300 ℃ as

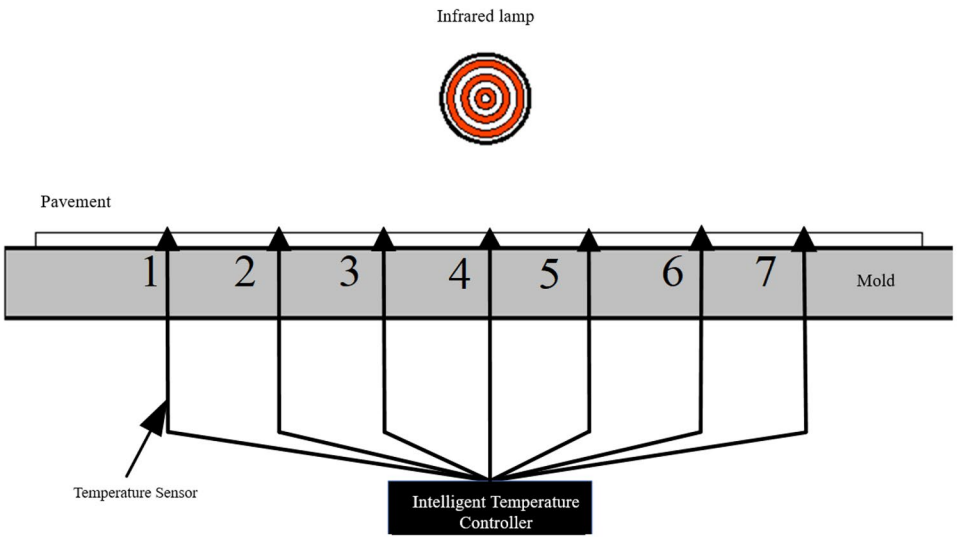

Fig. 18 Layout of preheating infrared lamps

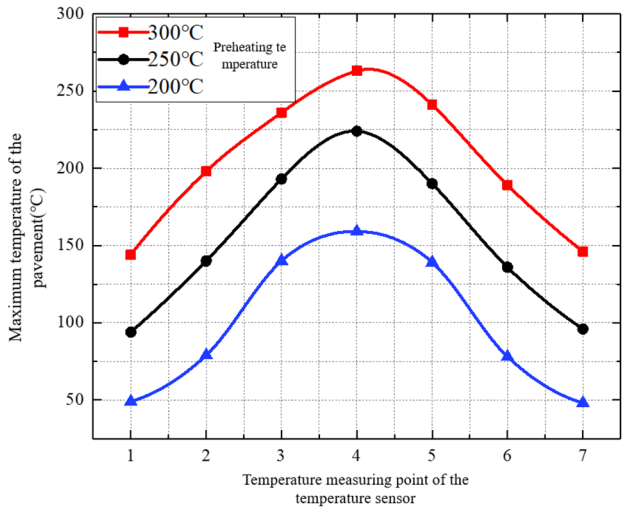

Fig. 19 The influence of preheating temperature on the horizontal direction of the pavement

an example, the temperature sensor no. 4 in the center of the heating, the measured temperature is 272 ℃, which is an 11℃ increase relative to that under the single lamp. The temperature difference between the single and dual heat sources gradually expanded as it moved away from the center of the heat source. Under double preheating, the temperature change is smoother relative to that under a single lamp, and the radiation range is expanded by increasing the lamp to make the temperature more uniform, thus improving the preheating effect.

In the previous paper, it was determined that the glass transition temperature of PEEK is about 143 °C. Therefore, according to the results of the IR lamp experiment, the preheating at 200 °C can ensure that the layup temperature can be maintained at about 140 °C within the radiation range of the IR lamp to ensure the crystallinity of the filament bundle, so the subsequent preheating temperature of 200 °C was chosen for the layup.

2.6.3 Influence of hot air heating parameters

The study of the influence law of hot air is mainly analyzed by the influence produced by hot air on the same paving layer. As shown in Fig. 21, six groups of temperature sensors are discharged in order, as shown in Fig. 21, where point 1 is the melting point and points 2–5 are lined up in order to the left according to a distance of 5 mm.

(1) The influence of distance on heating

The heat loss of the heat gun is relatively serious compared with other heat sources, and the heating distance is a relatively important influencing factor. Therefore, two sets of distances of 10 mm and 20 mm are selected in this paper. Take the no. 1 temperature measurement point as an example, and analyze the influence of different heating distances on the melting point of the pavement under different temperatures. The experimental results are shown in Fig. 22.

According to the histogram, it can be seen that the temperature loss of the hot air measured by the temperature sensor at the melting point is more than 10 ℃. When the distance of the hot air gun continues to increase the distance to 20 mm, the temperature loss of the hot air gun is between

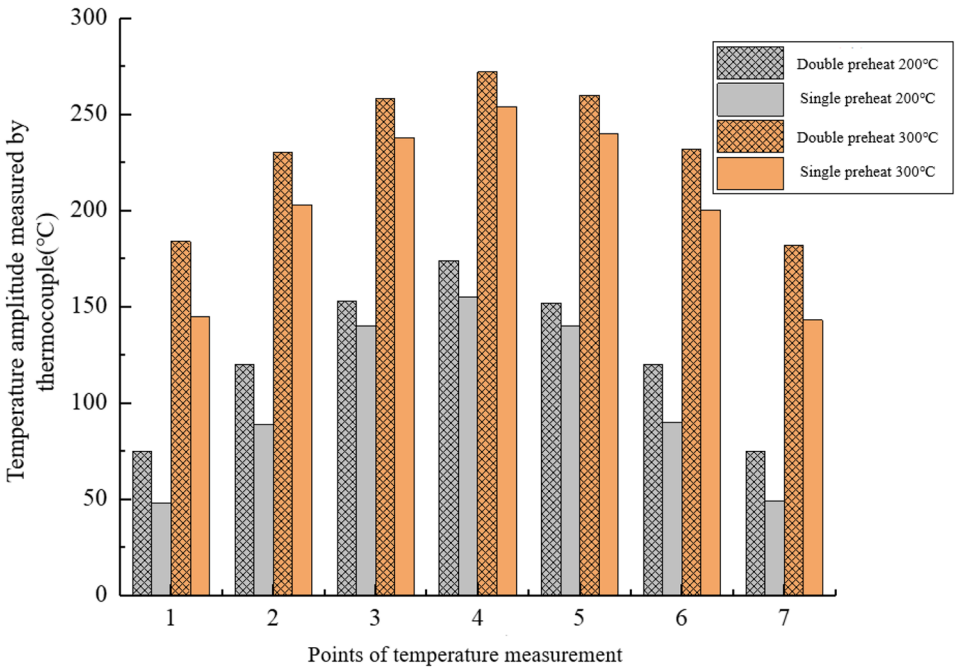

Fig. 20 The influence of the number of preheating heat sources on the ply

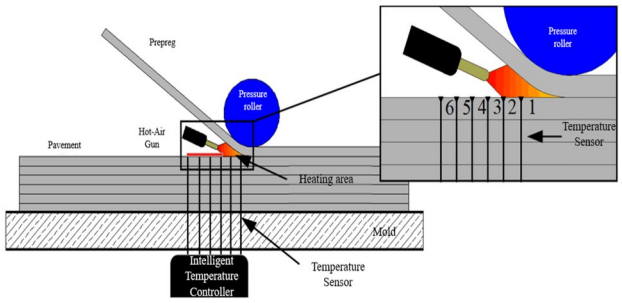

Fig. 21 Schematic diagram of the layout of the horizontal hot air experiment

30 and 40 ℃. Therefore, when laying, the range is controlled within 10 mm to ensure heating efficiency.

(2) The influence of hot air on horizontal motion

The temperature change curve obtained from the experiment is shown in Fig. 23, and it can be seen that the curve on the upper side is the temperature collected by the six temperature measurement points within 10 mm of the melting point of the hot air gun, with the highest temperature collected by the temperature sensor no. 1 being 485 °C. The temperature sensor no. 2 can still be affected by the hot air, but the temperature obtained has dropped below. The distance between the hot air gun and point 1 and other temperature measurement points is greater, in 3–6 points, basically not affected by the hot air gun. The convection area mentioned in the previous article is directly heated by hot air, so the pavement temperature easily reaches the melting temperature. Compared with the natural convection area, the temperature difference gradient is larger. Therefore, it is

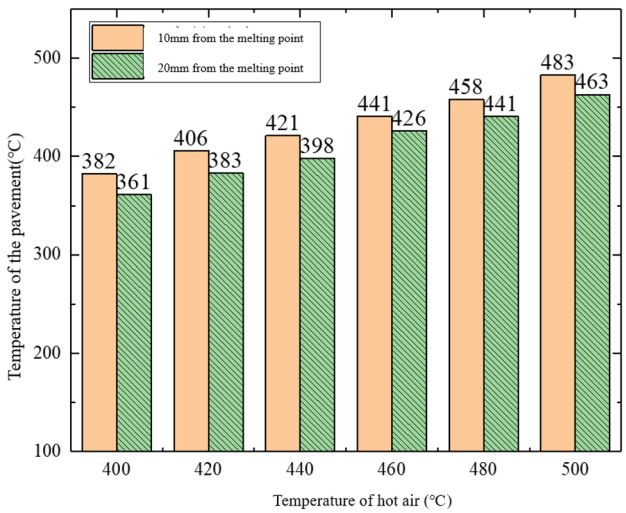

Fig. 22 The influence of hot air distance on paving at different temperatures

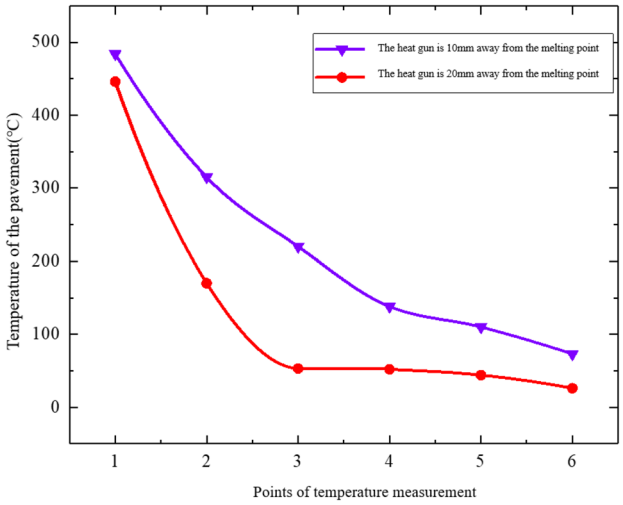

Fig. 23 The influence of the distance of the hot air gun on the horizontal direction

important to reduce the temperature gradient by preheating the pavement base before entering the influence of hot air to improve the heating efficiency.

(1) The effect of wind speed

Using the hot air gun as the heat source for carbon fiber forming, it is necessary to consider the effect of wind speed on its forming. In this paper, we analyze the influence law of hot air on different layups between different horizontal directions at different wind speeds, and the analysis results are shown in Fig. 24.

The heat gun selected in this paper is an air-pump type heat gun with a large and stable wind speed range. The wind test instrument was used to determine the calibration of the

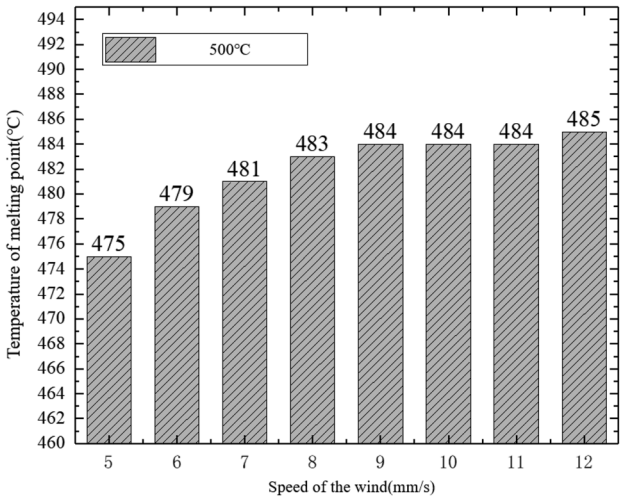

Fig. 24 The influence of different wind speeds on the same pavement

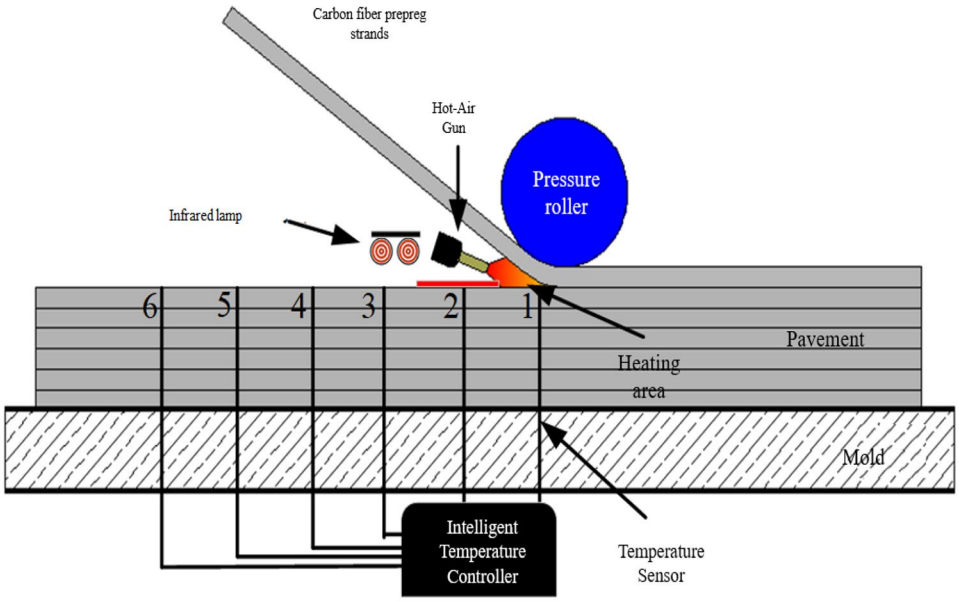

Fig. 25 Schematic diagram of sensor layout

heat gun to determine the wind speed range of 5 ~ 12 mm/s. Eight wind speed points were determined to analyze the temperature change law of the pavement surface under different wind speeds. The heating temperature was set to 500 ℃, and the heating wind speed was recorded at 5 ~ 12 m/s temperature variation.

According to the histogram, it can be seen that in the selected wind speed range, the temperature shows an increase with the gradual increase of wind speed. However, the surface temperature of the laying layer does not change significantly with the change in wind speed. In the actual measurement, the measured temperature is the temperature measured after the temperature is kept stable. The heating time of the surface of the filament bundle is inversely proportional to the wind speed, and the heating time of the heat source on the surface of the pavement is relatively lower as the wind speed gradually increases. At high wind speeds, the warming speed is faster and the temperature is higher, so a wind speed of 12 mm/s is chosen for the subsequent layup.

2.6.4 Temperature change of the pavement during automatic layup

Through the experimental analysis in the previous section, the influence laws of the hot air gun and infrared lamp as heat sources and preheat heat sources, respectively, in the temperature field were determined. Therefore, this

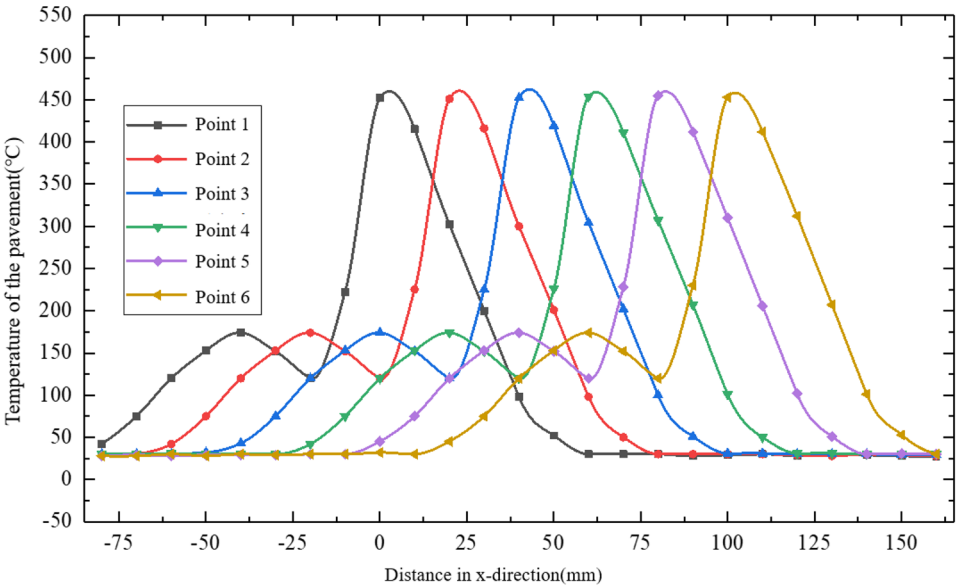

Fig. 26 Temperature changes during laying at six temperature points

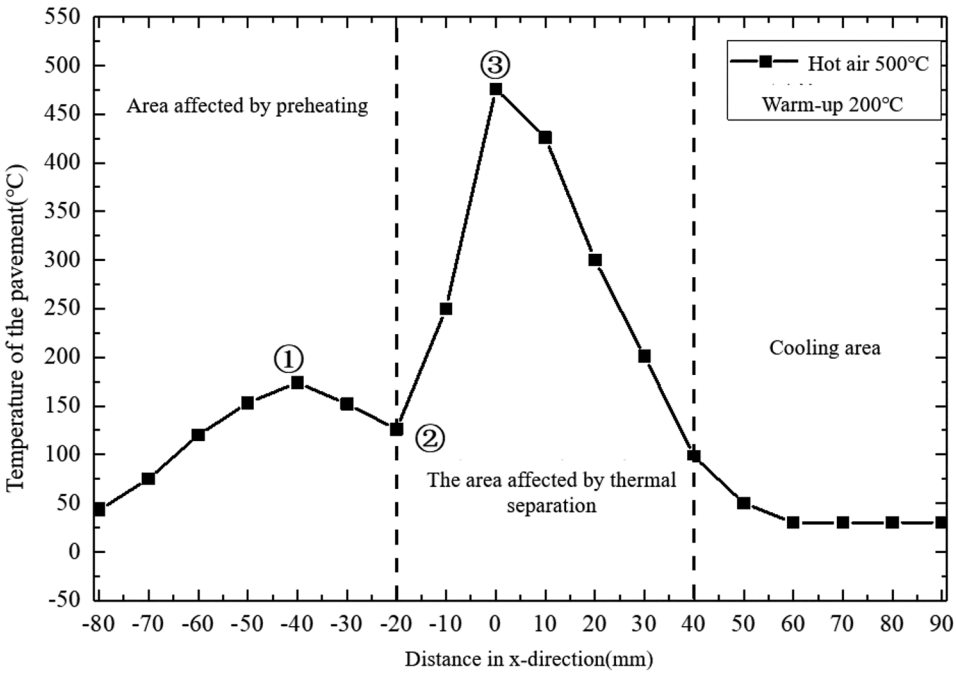

Fig. 27 Temperature change during the laying process of no. 1 point

subsection analyzes the effect of the infrared lamp preheating the prepreg filament bundle and the hot air heating the filament bundle on the layup at a layup speed of 5 mm/s.

(1) The effect of horizontal direction

For the analysis of the same layup, six groups of temperature sensors were arranged horizontally according to a spacing of 20 mm, and the schematic diagram of the device is shown in Fig. 25. In the experiment, the hot air temperature is set to 500 ℃, the lamp temperature is set to 200 ℃, the temperature measurement point no. 1 is defined as point 0, the laying direction is set to positive, and the temperature change curve of 6 points is measured when the laying head is moved to different points.

The temperature change curve of the six temperature points arranged horizontally is shown in Fig. 26. In the process of laying, according to the curve, it can be seen that the temperature change trend of the six points is the same under the simultaneous action of preheating and heating. Temperature fluctuations may occur at different points, but the change is small.

The curve variation at point 1 was analyzed as shown in Fig. 27. The temperature of hot air in the forced convection area and natural convection area was analyzed in the previous paper when analyzing hot air heating, so the preheating influence area and hot air influence area were divided according to the temperature change. In the preheating influence region, a process of temperature first decreasing and then rising appears in the curve, and in this region, point ① is the point where the paving head moves and the central area of the infrared lamp reaches the temperature measurement point, and an extreme value appears; because there is an air cooling zone when the lamp and the hot air gun are arranged, at point ②, the influence of preheating decreases because of preheating, while the influence of hot air is smaller, leading to the appearance of the temperature minima; and the air cooling zone is important. The air cooling zone has an important role in reducing the temperature gradient between the layup layers [18]. Thereafter, with the movement of the laying head, the temperature gradually increases as it enters the influence area of the hot air and reaches the larger value point

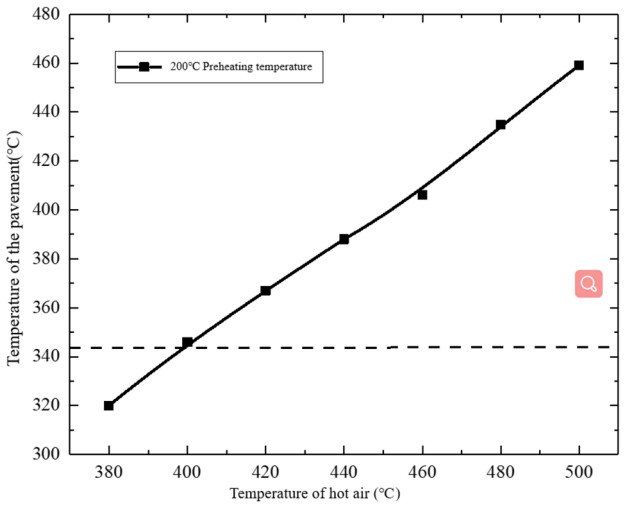

Fig. 28 Laying temperature changes of different hot air temperatures

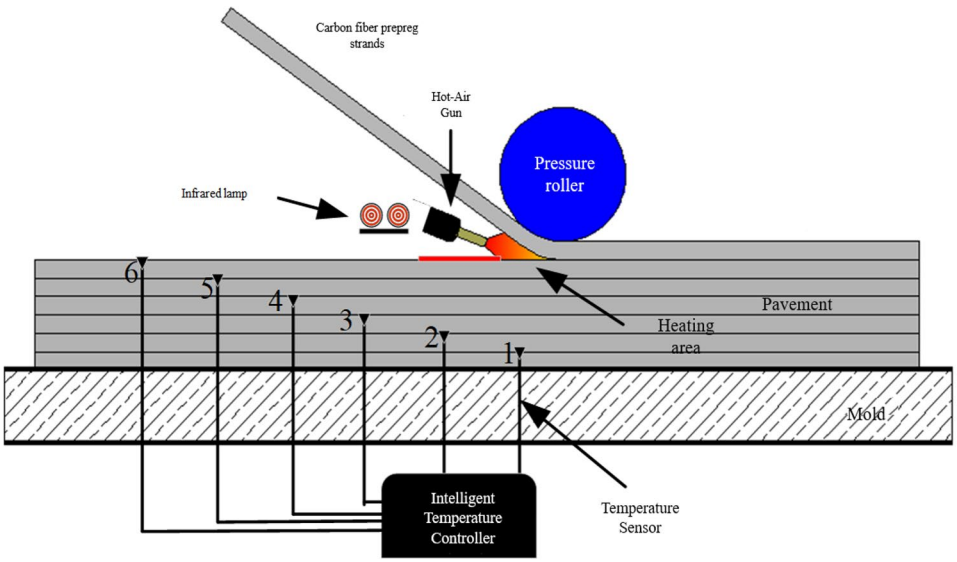

Fig. 29 Laying direction sensor layout diagram

③. With the movement of the laying head, the influence of the hot air gradually decreases, and finally the temperature at the temperature measurement point reaches the room temperature value.

At the same time, it is necessary to consider the influence of heating temperature on the layup during the layup process, so a preheating temperature of 200 °C was chosen to analyze the influence of temperature change on the layup in the range of 380–500 °C. According to the measured temperature values of 6 points, the average temperature was taken and the temperature variation curve was drawn as shown in Fig. 28.

According to the curve, it can be seen that controlling the hot air heating temperature above 400 °C can ensure that the layup temperature of the filament bundle reaches the melting point. Since the hot air loss is relatively serious, the specific hot air temperature depends on the air outlet cross section, air speed, layup distance, preheating, and etc. Hence, for this layup platform, it is necessary to control the temperature above 400 °C to ensure the normal layup and forming of the prepreg silk bundle. Therefore, to ensure the normal formation of the wire bundle, the temperature range chosen is 400 ~ 500 ℃.

(2) The effect of the vertical direction of the pavement

The temperature of the mold was set to 140 °C to study the temperature variation of different layers under different preheating temperatures. Six sets of temperature sensors were set up according to the layup direction to measure the temperature variation of each layer under different preheating temperatures according to the six layers from top to bottom, as shown in Fig. 29.

In the simulation analysis, the influence of preheating and hot air heating on the direction of the pavement was determined. Here, three preheating temperatures of 200 °C, 250 °C, and 300 °C were chosen to measure the temperature change curve of the pavement when the hot air temperature was 500 °C. The experimental results are shown in Fig. 30.

By observing the changes of the layup temperature curves at the three preheating temperatures, it can be seen that the temperature is closer at the first layup layer because it is subjected to a larger mold preheating temperature, and the temperature difference expands as the number of layup layers increases. At the same time, the temperature difference between the pavement layers gradually decreases with the increase in preheating temperature. The temperature of the plies at the three sets of preheating temperatures is close

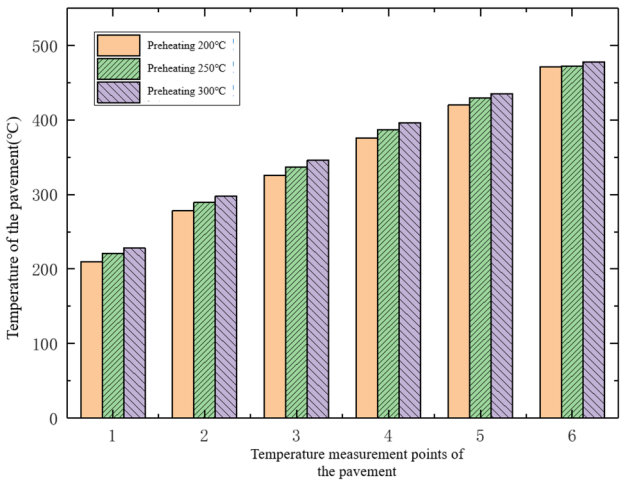

Fig. 30 Laminate temperature changes at different preheating temperatures

Table 10 Comparison table of experimental and simulated ply temperature

Layers	The preheating situation			
	Simulation of 200 ℃	Experiment 200 ℃	Experiment 250 ℃	Experiment 300 ℃
1	225	210	228	232
2	300	278	290	298
3	341	328	337	346
4	390	376	387	393
5	435	427	430	435
6	475	471	472	476

because it is close to the highest temperature of the hot air at that speed, and the effect produced by preheating becomes smaller. The simulation results are also compared with the experimental results, as shown in Table 10.

The comparison found that, at the same preheat temperature, the actual measured temperature change curve and the simulation to obtain the temperature change trend are similar. The simulation at 200 ℃ preheat temperature and the simulation at 300 ℃ preheat temperature are closer because the simulation will preheat idealized settings while the heat loss of the lamp, resulting in the temperature on the surface of the laying layer, is about 200 ℃ or more; the actual laying, because of the arrangement of the device and heat loss and other circumstances, leads to a deviation of the laying temperature. Combined with the previous analysis, a preheating temperature of 200 °C for the infrared lamp for layup can ensure the surface temperature of the filament bundle is the glass transition temperature.

3 Conclusions

The first layer of layup should be heated to 260 °C. The first layer of layup should be normal melting. In order to make the crystallinity of PEEK prepreg stable, it is necessary to use the method of variable process preheating. The other layers for layup should be set at 140 °C, and the high layup mold temperature should be set at 200 °C, according to a finite element analysis of the temperature field. Preheating the mold before to layup can help to reduce the temperature disparity between the layers and improve the molding effect.

Preheating trials with double infrared lamps show that the temperature change is smoother under double preheating than under single preheating, and the radiation range is enlarged by doubling the lamps, making the temperature more uniform and therefore improving the preheating effect. With a preheating temperature of 200 °C, the laying temperature may be maintained at around 140 °C within the infrared lamp's radiation range, ensuring the crystallinity of the filament bundle. Because hot air loss is more severe in the horizontal direction of laying, the specific hot air temperature is determined by the air outlet section, wind speed, laying distance, and preheating, among other factors. The temperature on this laying platform must be kept above 400 °C to guarantee proper laying and shaping of the prepreg silk bundle. The temperature range chosen to enable normal formation of the silk bundle is 400 ~ 500 °C. In the vertical direction of laying, at the same preheating temperature, the actual measured temperature change curve and the simulation to obtain the temperature change trend are similar. The simulation at 200 ℃ preheating temperature and the simulation at 300 ℃ preheating are closer, because the simulation will preheat idealized settings while the heat loss of the lamp, resulting in the temperature at the surface of the laying layer, is about 200 ℃ or more. The actual laying, because of the arrangement of the device and heat loss and other circumstances, resulting in the laying temperature deviation, can ensure that the surface temperature of the filament beam is at the glass transition temperature.

Author contribution All authors contributed to the study conception and design, all authors commented on previous versions of the manuscript, and all authors read and approved the final manuscript.

Funding The work is supported by the International Science and Technology Cooperation Program of Jiangsu Province (NO. BY2021540).

Availability of data and material All data generated or analyzed during this study are included in this article (and its supplementary information files).

Code availability Not applicable.

Declarations

Ethics approval There are no ethical issues involved in this article.

Consent to participate Not applicable.

Consent for publication Not applicable.

Competing interests The authors declare no competing interests.

References

1. Schmidt HC, Damerow U, Lauter C, Gorny B, Hankeln F, Homberg W et al (2012) Manufacturing processes for combined forming of multi-material structures consisting of sheet metal and local CFRP reinforcements. Key Eng Mater 504–506:295–300. https://doi.org/10.4028/www.scientific.net/KEM.504-506.295
2. Parry TV, Wronski S (1981) Selective reinforcement of an aluminium alloy by adhesive bonding with uniaxially aligned carbon

fibre/epoxy composites. Composites 12(4):249–255. https://doi.org/10.1016/0010-4361(81)90013-6
3. Broughton JG, Beevers A, Hutchinson AR (1997) Carbon-fibre-reinforced plastic (CFRP) strengthening of aluminium extrusions. Int J Adhes Adhes 17(3):269–278. https://doi.org/10.1016/S0143-7496(97)00020-1
4. Kim P (1998) A comparative study of the mechanical performance and cost of metal, FRP, and hybrid beams. Appl Compos Mater 5(3):175–87. https://doi.org/10.1023/A1008830017745
5. Coulter C, Richards R, Peterson D, Collier J (2014) Parietal skull reconstruction using immediate PEEK cranioplasty following resection for craniofacial fibrous dysplasia. J Plast Reconstr Aesthet Surg 67(8):208–209. https://doi.org/10.1016/j.bjps.2014.02.015
6. Zhu S, Qian Y, Hassan EAM, Shi R, Yang L et al (2020) Enhanced interfacial interactions by PEEK-grafting and coupling of acylated CNT for GF/PEEK composites. Compos Commun 18:43–48. https://doi.org/10.1016/j.coco.2020.01.008
7. Verma S, Sharma N, Kango S, Sharma S (2021) Developments of PEEK (Polyetheretherketone) as a biomedical material: a focused review. Eur Polymer J 147:110295. https://doi.org/10.1016/j.eurpolymj.2021.110295
8. Zhang J, Tian W, Chen J, Yu J, Zhang J, Chen J (2019) The application of polyetheretherketone (PEEK) implants in cranioplasty. Brain Res Bull 153:143–149. https://doi.org/10.1016/j.brainresbull.2019.08.010
9. Czaderski C, Martinelli E, Michels J, Motavalli M (2012) Effect of curing conditions on strength development in an epoxy resin for structural strengthening. Compos B Eng 43(2):398–410. https://doi.org/10.1016/j.compositesb.2011.07.006
10. Benedetti A, Fernandes P, Granja JL, Sena-Cruz J, Azenha M (2016) Influence of temperature on the curing of an epoxy adhesive and its influence on bond behaviour of NSM-CFRP systems. Compos B Eng 89:219–229. https://doi.org/10.1016/j.compositesb.2015.11.034
11. Sorrentino L, Esposito L, Bellini C (2016) A new methodology to evaluate the influence of curing overheating on the mechanical properties of thick FRP laminates. Composites Part B: Engineering 109:187–96. https://doi.org/10.1016/j.compositesb.2015.11.034
12. Sonmez FO, Hahn HT (1997) Modeling of heat transfer and crystallization in thermoplastic composite tape placement process. J Thermoplast Compos Mater 10(3):198–240. https://doi.org/10.1177/089270579701000301
13. Stokes-Griffin CM, Compston P (2015) A combined optical-thermal model for near-infrared laser heating of thermoplastic composites in an automated tape placement process. Compos A Appl Sci Manuf 75:104–115. https://doi.org/10.1016/j.compositesa.2014.08.006
14. Grouve WJB (2017) Weld strength of laser-assisted tape-placed thermoplastic composites. University of Twente
15. Lundström F, Frogner K, Andersson M (2020) A numerical model to analyse the temperature distribution in cross-ply CFRP during induction heating. Compos B Eng 202:108419. https://doi.org/10.1016/j.compositesb.2020.108419
16. Kollmannsberger A, Lichtinger R, Hohenester F, Ebel C, Drechsler K (2018) Numerical analysis of the temperature profile during the laser-assisted automated fiber placement of CFRP tapes with thermoplastic matrix. J Thermoplast Compos Mater 31(12):1563–1586. https://doi.org/10.1177/0892705717738304
17. Stokes-Griffin CM, Kollmannsberger A, Heard S, Compston P, Drechsler K (2018) Manufacture of steel–CF/PA6 hybrids in a laser tape placement process: effect of first-ply placement rate on thermal history and lap shear strength. Compos A Appl Sci Manuf 111:42–53. https://doi.org/10.1016/j.compositesa.2018.05.007
18. Heider D, Piovoso MJ, Gillespie Jr JW (2002) Application of a neural network to improve an automated thermoplastic tow-placement process. J Process Control 12(1):101–111. https://doi.org/10.1016/S0959-1524(00)00064-0
19. Tierney J, Gillespie JW (2006) Modeling of In situ strength development for the thermoplastic composite tow placement process. J Compos Mater 40(16):1487–1506. https://doi.org/10.1177/0021998306060162
20. Stokes-Griffin CM, Matuszyk TI, Compston P, Cardew-Hall MJ (2012) Modelling the automated tape placement of thermoplastic composites with in-situ consolidation.5 Sustainable Automotive Technologies 2012:61–68. https://doi.org/10.1007/978-3-642-24145-1_9
21. Heider D, Piovoso MJ, Gillespie JW (2003) A neural network model-based open-loop optimization for the automated thermoplastic composite tow-placement system. Compos A Appl Sci Manuf 34(8):791–799. https://doi.org/10.1016/S1359-835X(03)00120-9
22. Gain AK, Oromiehie E, Gangadhara PB (2022) Nanomechanical characterisation of CF-PEEK composites manufactured using automated fibre placement (AFP). Composites Communications 31:101109. https://doi.org/10.1016/j.coco.2022.101109